

Bayesian Nonparametric Inference for Panel Count Data with an Informative Observation Process

Ye Liang¹, Yang Li² and Bin Zhang³

¹ *Department of Statistics, Oklahoma State University, Stillwater, OK 74074*

² *Department of Mathematics and Statistics, University of North Carolina, Charlotte, NC 28223*

³ *Division of Biostatistics and Epidemiology, Cincinnati Children's Hospital, Cincinnati, OH 45229*

Abstract

In this paper, the panel count data analysis for recurrent events is considered. Such analysis is useful for studying tumor or infection recurrences in both clinical trial and observational studies. A bivariate Gaussian Cox process model is proposed to jointly model the observation process and the recurrent event process. Bayesian nonparametric inference is proposed for simultaneously estimating regression parameters, bivariate frailty effects and baseline intensity functions. Inference is done through Markov chain Monte Carlo, with fully developed computational techniques. Predictive inference is also discussed under the Bayesian setting. The proposed method is shown to be efficient via simulation studies. A clinical trial dataset on skin cancer patients is analyzed to illustrate the proposed approach.

Keywords: Nonhomogeneous Poisson process; Gaussian process; Recurrent event; Dependent frailty; Hamiltonian Monte Carlo;

1 Introduction

Panel count data in medical studies often refer to incomplete recurrent event data observed only at finite distinct observation time points. The set of observation times may vary from subject to subject. Using mathematical notations, for subject i from a sample of n subjects, we observe the subject only at discrete time points: $t_{i,1}, \dots, t_{i,m_i}$, where m_i is the total number of observations for subject i . At any time point $t_{i,j}$, we observe a cumulative count $N_{i,j}$ of a recurrent event, but the actual event times are unknown. A classical example of panel count data is the bladder tumor data (Sun and Wei, 2000). In the study, a list of post-surgical patients were assigned to three treatment groups. Each patient had multiple random clinical visits and the number of recurrent tumors between two visits were observed. Another example was a chemotherapy trial for skin cancer patients (Li et al., 2011). In the

study, two treatment groups of patients were followed up at clinical visits and the number of recurrent non-melanoma skin cancers were observed. Other examples include infection recurrences in leukemia patients and respiratory system exacerbations among cystic fibrosis patients (Kalbfleisch and Prentice, 2011).

One common approach for modeling panel count data is to regard the underlying recurrent event process as a counting process, for instance, the nonhomogeneous Poisson process. For regression analysis of panel count data, the Cox model is a popular choice (Anderson and Gill, 1982), where covariates and a baseline intensity function are specified in a log-linear form. Recently, there has been an increasing attention in literature on the dependence between the observation process and the recurrent event process, for which a bivariate joint modeling seems a natural approach. Such bivariate models usually assume dependence specified through subject-specific frailties. He et al. (2009); Huang et al. (2006); Sun et al. (2007) proposed joint modeling approaches that depend on shared random effects. Li et al. (2010) proposed a class of semiparametric transformation models. Li et al. (2015) proposed a semiparametric regression model in which the underlying dependence structure for random effects are unspecified. Zhao, Li and Sun (2013); Zhou et al. (2016) combined such context with terminal events.

For all existing bivariate joint modeling that we are aware of, estimation on regression parameters was primarily focused but estimation on baseline intensity functions was rarely considered for the nature of Cox model and its generalizations. However, a smooth estimate of baseline functions may still be useful in terms of comprehension and prediction, to both physicians and patients. Altman and Royston (2000); Royston and Altman (2013) have argued this point for baseline hazard functions in survival analysis. On the other hand, previous research work on baseline estimation predominantly used spline-based models (Nielsen and Dean, 2008; Lu et al., 2007, 2009; Hua and Zhang, 2012; Hua et al., 2014; Yao et al., 2016), but without considering a dependent observation process. It remains unclear how these spline-based methods can be extended to cases where the observation process is correlated.

In this paper, we consider a bivariate joint modeling for panel count data when the observation and event processes are dependent. Our main goal is to provide an inferential procedure that can simultaneously estimate regression coefficients and baseline intensity functions while allowing for correlated processes. For this purpose, we propose a log-Gaussian Cox process model under the Bayesian framework, which can be shown more flexible than existing models. In addition, we develop a nonparametric Bayesian inference through Markov chain Monte Carlo (MCMC) for the proposed model. With the proposed Bayesian inference,

we can estimate both the intensity function and the mean function, and furthermore, do predictive inference on disease recurrences for future patients.

The rest of this paper is organized as follows. Section 2 describes the model specification, especially the log-Gaussian Cox process. Section 3 establishes the inference framework, including Bayesian inference and posterior sampling steps. Section 4 describes Bayesian predictive inference using posterior samples. Section 5 presents results from extensive simulation studies, where our method is compared with several existing methods. In Section 6, the proposed method is applied to a clinical trial dataset on a skin cancer treatment. Section 7 is a discussion on future directions.

2 The Model

2.1 The log-Gaussian Cox process model

Suppose we observe subject i at distinct time points t_{ij} , $j = 1, \dots, m_i$ and $i = 1, \dots, n$. At each time point t_{ij} , we observe a cumulative count N_{ij} of the recurrent event. We note that the underlying observation process $\{T_i(t), t \in \mathbb{R}\}$ and the event process $\{N_i(t), t \in \mathbb{R}\}$ are dependent. Suppose $\{T_i(t), t \in \mathbb{R}\}$ follows a nonhomogeneous Poisson process with intensity function $\mu_i(t)$ and we consider a Cox regression model,

$$\mu_i(t) = \mu_0(t) \exp\{\mathbf{x}'_i \boldsymbol{\gamma}\} u_i^O, \quad (1)$$

where $\mu_0(t)$ is the baseline intensity function, \mathbf{x}_i are covariates and u_i^O is a subject-specific frailty. We also assume that the event process $\{N_i(t), t \in \mathbb{R}\}$ is a nonhomogeneous Poisson processes with intensity function $\lambda_i(t)$ given by

$$\lambda_i(t) = \lambda_0(t) \exp\{\mathbf{x}'_i \boldsymbol{\beta}\} u_i^N, \quad (2)$$

where $\lambda_0(t)$ is the baseline intensity function and u_i^N is a frailty that is correlated with u_i^O .

Since both $\mu_0(t)$ and $\lambda_0(t)$ are non-negative random functions, it is natural to consider a logarithm transformation so that the resulting functions can take unrestricted values. Assume that $\mu_0(t) = \exp\{g_1(t)\}$ and $\lambda_0(t) = \exp\{g_2(t)\}$, where each of $\{g_1(t) : t \in \mathbb{R}\}$ and $\{g_2(t) : t \in \mathbb{R}\}$ is a stationary Gaussian process, with constant means γ_0 and β_0 , covariance functions $C_1(h) = \text{Cov}\{g_1(t), g_1(t+h)\}$ and $C_2(h) = \text{Cov}\{g_2(t), g_2(t+h)\}$, i.e.

$$g_1(t) \sim \text{GP}(\gamma_0, C_1(h)) \quad \text{and} \quad g_2(t) \sim \text{GP}(\beta_0, C_2(h)). \quad (3)$$

Notice that $\mathbf{x}'_i\boldsymbol{\gamma}$ and $\mathbf{x}'_i\boldsymbol{\beta}$ should not contain intercept terms to avoid identifiability problems. This specification on $\mu_0(t)$ and $\lambda_0(t)$ actually gives us Cox processes, which is defined by assuming the intensity function of a nonhomogeneous Poisson process from a nonnegative-valued stochastic process. The Cox process is also known as a doubly stochastic Poisson process. In our proposed model, we in fact have a log-Gaussian Cox process (Møller et al., 1998), with the log-intensity function being Gaussian. Given that spline models have been predominantly used for panel count data analysis, it should be noted that the equivalence between splines and Gaussian processes is known as early as Kimeldorf and Wahba (1970). Spline models can be viewed as special Gaussian processes with certain kernels. One advantage of Gaussian processes is that one no longer needs to consider the knots placement, which, on the other hand, is crucial for spline models (Rasmussen and Williams, 2006).

We give the following moment properties for subject specific intensity functions as follows. Under the specified log-Gaussian Cox process model, given $\boldsymbol{\gamma}$, $\boldsymbol{\beta}$, u_i^N and u_i^O ,

$$\begin{aligned} \text{E}\{\mu_i(t)\} &= \exp\left\{\mathbf{x}'_i\boldsymbol{\gamma} + \frac{C_1(0)}{2}\right\} u_i^O, \\ \text{E}\{\lambda_i(t)\} &= \exp\left\{\mathbf{x}'_i\boldsymbol{\beta} + \frac{C_2(0)}{2}\right\} u_i^N, \\ \text{Cov}\{\mu_i(t), \mu_i(t+h)\} &= [\text{E}\{\mu_i(t)\}]^2 [\exp\{C_1(h)\} - 1], \\ \text{Cov}\{\lambda_i(t), \lambda_i(t+h)\} &= [\text{E}\{\lambda_i(t)\}]^2 [\exp\{C_2(h)\} - 1]. \end{aligned}$$

2.2 Frailty model

A correlated frailty model is commonly used to model the bivariate dependence (Sun et al., 2007; Li et al., 2011; Zhao, Tong and Sun, 2013; Li et al., 2015). A link function between u_i^O and u_i^N is often assumed, for example, $u_i^N = (u_i^O)^\alpha$, where α apparently controls the dependence. One limitation is that the link function needs to be pre-specified and how to choose a good one is unclear. Another arguably more serious limitation, is that a link function may lead to unappealing properties. For the link function considered above, the parameter α will be zero in the case of independence, which forces $u_i^N = 1$ for all subjects and thus fails to model the subject-dependent variation.

A better alternative is to consider a bivariate distribution for (u_i^O, u_i^N) . Let $(\log u_i^O, \log u_i^N)' = (z_{1i}, z_{2i})' = \mathbf{z}_i$ be a bivariate normal distribution $\mathbf{z}_i \sim N_2(\mathbf{0}, \mathbf{D})$, where the mean is restricted to be zero to avoid identifiability problems. Equivalently, $(u_i^O, u_i^N)'$ follows a bivariate log-normal distribution (Mostafa and Mahmoud, 1964). Following a straightforward calculation,

the cross covariance between $\mu_i(t)$ and $\lambda_i(t)$, given $\boldsymbol{\gamma}$ and $\boldsymbol{\beta}$ is now

$$\text{Cov}\{\mu_i(t), \lambda_i(t+h)\} = \text{E}\{\mu_i(t)\}\text{E}\{\lambda_i(t)\}(e^{D_{12}} - 1),$$

in which, D_{12} controls the dependence between the two processes.

2.3 Covariance functions and hyper-priors

The theoretical requirement for the covariance function $C(h)$ is that any covariance matrix constructed by it be positive-definite. Let $C(h) = \sigma^2 r(h)$, where $r(h)$ is a parametric correlation function (or called a Gaussian kernel). The Gaussian process is flexible with various choices of kernels. We consider the widely used Matérn kernel:

$$r(h) = 1/2^{\nu-1}\Gamma(\nu) (|h|/\theta)^\nu K_\nu (|h|/\theta),$$

where $K_\nu(\cdot)$ is the modified Bessel function of order ν and θ is the scale parameter. The shape parameter ν is often pre-specified for a desired differentiability of the curve. When $\nu = 1/2$, the Matérn kernel reduces to the exponential kernel $r(h) = \exp\{-|h|/\theta\}$, and when $\nu \rightarrow \infty$, the Matérn kernel goes to the squared exponential kernel $r(h) = \exp\{-|h|^2/\theta^2\}$.

Lastly, we specify hyper-priors for the remaining parameters in the model. Let the regression coefficients have noninformative priors: $\pi(\boldsymbol{\gamma}) \propto 1$ and $\pi(\boldsymbol{\beta}) \propto 1$. Let the frailty covariance \mathbf{D} be inverse-Wishart: $\mathbf{D} \sim \text{IWish}(k_0, \mathbf{V}_0)$, with $k_0 = 3$ and $\mathbf{V}_0 = \text{diag}\{1\}$, so that this prior is only weakly informative. For hyperparameters in $C_1(h)$ and $C_2(h)$, let σ_k^2 , $k = 1, 2$, be inverse gamma: $\sigma_k^2 \sim \text{IG}(a_0, b_0)$, with $a_0 = b_0 = 1$. The priors on the length-scales θ_k are chosen to be informative gamma priors based on empirical evidences (Diggle et al., 2013).

3 Bayesian Inference

3.1 The joint posterior distribution

With the full Bayesian model specified in Section 2, we now give inference and computation details. For each subject i , we observe a complete realization of the observation process $T_i(t)$: $t_{i,1}, \dots, t_{i,m_i}$, up to a given follow-up time C_i . Under the Poisson process assumption,

the likelihood function for observation times is

$$\begin{aligned} L_1(\mu_0(\cdot), \boldsymbol{\gamma}, \mathbf{w}; \mathbf{t}) &= \prod_{i=1}^n m_i! p(m_i) p(t_{i,1}, \dots, t_{i,m_i} | m_i) \\ &= \prod_{i=1}^n \left\{ e^{-\int_0^{C_i} \mu_0(s) \exp\{\mathbf{x}'_i \boldsymbol{\gamma}\} u_i^O ds} \prod_{j=1}^{m_i} \mu_0(t_{ij}) \exp\{\mathbf{x}'_i \boldsymbol{\gamma}\} u_i^O \right\}. \end{aligned}$$

Then for each event process $N_i(t)$, we observe cumulative counts given a realized $T_i(t)$. Let $y_{ij} = N_{ij} - N_{i,j-1}$ be the increment at time t_{ij} . The likelihood function for the increments, conditional on \mathbf{t} , is

$$\begin{aligned} L_2(\lambda_0(\cdot), \boldsymbol{\beta}, \mathbf{u}; \mathbf{y} | \mathbf{t}) &= \prod_{i=1}^n \prod_{j=1}^{m_i} \text{Poi} \left(y_{ij}; \int_{t_{i,j-1}}^{t_{ij}} \lambda_0(s) \exp\{\mathbf{x}'_i \boldsymbol{\beta}\} u_i^N ds \right) \\ &= \prod_{i=1}^n \prod_{j=1}^{m_i} \left[\left\{ \int_{t_{i,j-1}}^{t_{ij}} \lambda_0(s) \exp\{\mathbf{x}'_i \boldsymbol{\beta}\} u_i^N ds \right\}^{y_{ij}} e^{-\int_{t_{i,j-1}}^{t_{ij}} \lambda_0(s) \exp\{\mathbf{x}'_i \boldsymbol{\beta}\} u_i^N ds} / y_{ij}! \right]. \end{aligned}$$

Then the joint likelihood function $L(\mu_0(\cdot), \lambda_0(\cdot), \boldsymbol{\gamma}, \boldsymbol{\beta}, \mathbf{u}^O, \mathbf{u}^N; \mathbf{t}, \mathbf{y}) = L_1 \times L_2$. With priors specified in Section 2, the joint posterior distribution is given by

$$\begin{aligned} p(\boldsymbol{\gamma}, \boldsymbol{\beta}, \mathbf{u}^O, \mathbf{u}^N, \mathbf{D}, g_1(\cdot), g_2(\cdot), \sigma_1^2, \sigma_2^2, \theta_1, \theta_2 | \mathbf{t}, \mathbf{y}) &\propto L \times \pi(\boldsymbol{\gamma}) \times \pi(\boldsymbol{\beta}) \times \pi(\mathbf{u}^O, \mathbf{u}^N | \mathbf{D}) \\ &\times \pi(\mathbf{D}) \times \text{GP}(g_1(\cdot) | \sigma_1^2, \theta_1) \times \text{GP}(g_2(\cdot) | \sigma_2^2, \theta_2) \times \pi(\sigma_1^2, \sigma_2^2, \theta_1, \theta_2). \end{aligned}$$

3.2 Gibbs sampling

Inference on the posterior distribution is done computationally using MCMC. Consider a Gibbs sampling for the overall procedure. The full conditional distributions are discussed as follows.

For regression coefficients $\boldsymbol{\gamma}$ and $\boldsymbol{\beta}$, the full conditional distributions are

$$p(\boldsymbol{\gamma} | \text{rest}) \propto \exp \left\{ \sum_{i=1}^n \left(m_i \mathbf{x}'_i \boldsymbol{\gamma} - e^{\mathbf{x}'_i \boldsymbol{\gamma}} u_i^O \int_0^{C_i} e^{g_1(s)} ds \right) \right\} \quad (4)$$

and

$$p(\boldsymbol{\beta} | \text{rest}) \propto \exp \left\{ \sum_{i=1}^n \left(N_{i,m_i} \mathbf{x}'_i \boldsymbol{\beta} - e^{\mathbf{x}'_i \boldsymbol{\beta}} u_i^N \int_0^{t_{i,m_i}} e^{g_2(s)} ds \right) \right\}. \quad (5)$$

It is straightforward to show that both (4) and (5) are log-concave. Hence the adaptive rejection sampling (ARS) (Gilks and Wild, 1992) applies.

The full conditional distributions for the intercepts γ_0 and β_0 are

$$\gamma_0 \mid \text{rest} \sim N\left(\frac{\mathbf{1}'\boldsymbol{\Omega}_1\mathbf{g}_1}{\mathbf{1}'\boldsymbol{\Omega}_1\mathbf{1}}, \frac{1}{\mathbf{1}'\boldsymbol{\Omega}_1\mathbf{1}}\right) \quad \text{and} \quad \beta_0 \mid \text{rest} \sim N\left(\frac{\mathbf{1}'\boldsymbol{\Omega}_2\mathbf{g}_1}{\mathbf{1}'\boldsymbol{\Omega}_2\mathbf{1}}, \frac{1}{\mathbf{1}'\boldsymbol{\Omega}_2\mathbf{1}}\right) \quad (6)$$

where $\mathbf{1}$ is the vector of ones and $\boldsymbol{\Omega}_k$, $k = 1, 2$, is the corresponding covariance matrix for $g_k(\cdot)$, which will be discussed in the next sub-section.

For the frailties u_i^O and u_i^N and their covariance matrix \mathbf{D} , we instead update \mathbf{z}_i to avoid the lognormal density. Then the full conditional distribution for \mathbf{z}_i is

$$p(\mathbf{z}_i \mid \text{rest}) \propto \exp\left\{-\frac{1}{2}\mathbf{z}_i'\mathbf{D}^{-1}\mathbf{z}_i + z_{1i}m_i + z_{2i}N_{i,m_i} - e^{z_{1i}+\mathbf{x}_i'\boldsymbol{\gamma}} \int_0^{C_i} e^{g_1(s)} ds - e^{z_{2i}+\mathbf{x}_i'\boldsymbol{\beta}} \int_0^{t_{i,m_i}} e^{g_2(s)} ds\right\}. \quad (7)$$

Again, it is straightforward to show the log-concavity of this conditional density and the ARS is used for sampling \mathbf{z}_i . The full conditional distribution for \mathbf{D} is

$$\mathbf{D} \mid \text{rest} \sim \text{Inv-Wishart}\left(n + k_0, \sum_{i=1}^n \mathbf{z}_i\mathbf{z}_i' + \mathbf{V}_0\right). \quad (8)$$

For sampling the latent Gaussian process components $g_1(\cdot)$ and $g_2(\cdot)$, and their hyperparameters σ_1^2 , σ_2^2 , θ_1 and θ_2 , we have the following full conditional distributions:

$$p(g_1(\cdot) \mid \text{rest}) \propto \text{GP}(g_1(\cdot) \mid \sigma_1^2, \theta_1) \left\{ \prod_{i=1}^n \prod_{j=1}^{m_i} e^{g_1(t_{ij})} \right\} \exp\left\{-\sum_{i=1}^n e^{\mathbf{x}_i'\boldsymbol{\gamma}} u_i^O \int_0^{C_i} e^{g_1(s)} ds\right\}, \quad (9)$$

and

$$p(g_2(\cdot) \mid \text{rest}) \propto \text{GP}(g_2(\cdot) \mid \sigma_2^2, \theta_2) \left\{ \prod_{i=1}^n \prod_{j=1}^{m_i} \left(\int_{t_{i,j-1}}^{t_{ij}} e^{g_2(s)} ds \right)^{y_{ij}} \right\} \exp\left\{-\sum_{i=1}^n e^{\mathbf{x}_i'\boldsymbol{\beta}} u_i^N \int_0^{t_{i,m_i}} e^{g_2(s)} ds\right\}. \quad (10)$$

This requires high dimensional sampling and will be discussed in the next sub-section.

3.3 Riemann manifold Hamiltonian Monte Carlo

Since $g_1(\cdot)$ and $g_2(\cdot)$ are infinitely dimensional, a finely spaced grid over the time region of interest (i.e. a discretization) is needed. For instance, consider a grid $\{s_l : l = 0, \dots, L\}$ that

covers the entire time period. A pre-defined grid will induce a finite multivariate normal distribution from the Gaussian process, say, $\mathbf{g}_1 = (g_1(1), \dots, g_1(L))' \sim N_L(\boldsymbol{\mu}_{g_1}, \boldsymbol{\Omega}_1)$ and $\mathbf{g}_2 = (g_2(1), \dots, g_2(L))' \sim N_L(\boldsymbol{\mu}_{g_2}, \boldsymbol{\Omega}_2)$. Without loss of generality, assume that the entire time region has length one. Then the cell length of the grid is $1/L$ and an observation time t_{ij} is approximated as its corresponding cell index: $\lceil t_{ij}L \rceil$. The intensity function within each cell is approximated by a constant function, and then any integral in (9) and (10) is approximated by

$$\int_{t_{i,j-1}}^{t_{ij}} e^{g_2(s)} ds = \frac{1}{L} \sum_{l=\lceil t_{i,j-1}L \rceil}^{\lceil t_{ij}L \rceil} e^{g_2(l)}.$$

Note that the choice of grid and L is completely arbitrary. The fineness of such grid only reflects a balance between computational complexity and the accuracy of the approximation (Diggle et al., 2013).

Consider the logarithm of the approximated conditional density of either (9) or (10), denoted by $\mathbb{L}_r(\mathbf{g})$. For a chosen dimension L , now it becomes a challenging problem to sample the high dimensional \mathbf{g} from an irregular $\mathbb{L}_r(\mathbf{g})$. While the traditional Metropolis-Hastings algorithms have low efficiency in such problems, there has been an increasing focus on gradient-based sampling techniques, such as Metropolis adjusted Langevin algorithm and Hamiltonian Monte Carlo (Neal, 2010). Despite efficiency gained in those algorithms, they both require careful tuning in the implementation. A recent promising sampling technique called Riemann manifold Hamiltonian Monte Carlo (RMHMC) (Girolami and Calderhead, 2011) greatly eases the burden of tuning. The RMHMC utilizes the Riemann geometry of the parameter space by incorporating a metric tensor, usually the Fisher information matrix, to the Hamiltonian dynamics. To show the efficiency of utilizing RMHMC in our application, we compare it with another widely used algorithm for Gaussian process sampling, called elliptical slice sampling. Figure 1 shows that the RMHMC converges almost immediately.

To implement the algorithm, analytical forms of the gradient $\nabla_{\mathbf{g}} \mathbb{L}_r(\mathbf{g})$ and the Fisher information matrix $-\mathbb{E}_{\mathbf{y}, \mathbf{g} | \boldsymbol{\theta}} [\nabla_{\mathbf{g}}^2 \mathbb{L}_r(\mathbf{g})]$ are both required. In our case, the gradient is analytically available for the approximated log-densities $\mathbb{L}_1(\mathbf{g}_1)$ and $\mathbb{L}_2(\mathbf{g}_2)$:

$$\nabla_{\mathbf{g}_1} \mathbb{L}_1(\mathbf{g}_1) = -\boldsymbol{\Omega}_1(\mathbf{g}_1 - \boldsymbol{\mu}_{g_1}) + \mathbf{f}_1 + \mathbf{q}_1 \circ \mathbf{e}_1,$$

where \circ is the Hadamard product, $\mathbf{e}_1 = L^{-1}(e^{g_1(1)}, \dots, e^{g_1(L)})'$, both \mathbf{f}_1 and \mathbf{q}_1 are L -

dimensional vectors with

$$f_{1,l} = \sum_{i=1}^n \sum_{j=1}^{m_i} I(l = \lceil t_{ij}L \rceil),$$

$$q_{1,l} = - \sum_{i=1}^n \exp(\mathbf{x}'_i \boldsymbol{\gamma}) u_i^O I(l \leq \lceil C_i L \rceil),$$

for $l = 1, \dots, L$. On the other hand, we have

$$\nabla_{\mathbf{g}_2} \mathbb{L}_2(\mathbf{g}_2) = -\boldsymbol{\Omega}_2(\mathbf{g}_2 - \boldsymbol{\mu}_{g_2}) + \mathbf{0} + \mathbf{q}_2 \circ \mathbf{e}_2,$$

where $\mathbf{e}_2 = L^{-1}(e^{g_2(1)}, \dots, e^{g_2(L)})'$, and \mathbf{q}_2 is an L -dimensional vector with

$$q_{2,l} = L \sum_{i=1}^n \sum_{j=1}^{m_i} \frac{y_{ij} I(\lceil t_{i,j-1}L \rceil \leq l \leq \lceil t_{ij}L \rceil)}{\sum_{l=\lceil t_{i,j-1}L \rceil}^{\lceil t_{ij}L \rceil} e^{g_2(l)}} - \sum_{i=1}^n \exp(\mathbf{x}'_i \boldsymbol{\beta}) u_i^N I(l \leq \lceil t_{i,m_i}L \rceil),$$

for $l = 1, \dots, L$. For either \mathbb{L}_1 or \mathbb{L}_2 , the Fisher information matrix is analytically too complicated, but can eventually be expressed as $-\mathbb{E}_{\mathbf{y}, \mathbf{g} | \boldsymbol{\theta}} [\nabla_{\mathbf{g}}^2 \mathbb{L}(\mathbf{g})] = \boldsymbol{\Omega}^{-1} + \boldsymbol{\Lambda}/L$, where $\boldsymbol{\Lambda}$ has a complicated form. As L goes large, the second term is negligible. Therefore, $\boldsymbol{\Omega}^{-1}$ roughly is the desired metric tensor and is used as the mass matrix in Hamiltonian dynamics for both cases. Note, even if $\boldsymbol{\Omega}^{-1}$ is not sufficiently close to the actual metric tensor, the HMC algorithm is still valid because the mass matrix can be any matrix in theory. The rough use is only a matter of efficiency, not validity.

Hyperparameters $\sigma_1^2, \sigma_2^2, \theta_1$ and θ_2 in the Gaussian process are sampled alternately from $p(\sigma_k^2 | \text{rest}) \propto N(\mathbf{g}_k | \sigma_k^2, \theta_k) \pi(\sigma_k^2)$ and $p(\theta_k | \text{rest}) \propto N(\mathbf{g}_k | \sigma_k^2, \theta_k) \pi(\theta_k)$, $k = 1, 2$, where the former one is inverse gamma and the latter one is sampled by the adaptive rejection Metropolis sampling.

4 Prediction

Prediction is often considered an important part in ordinary linear regressions and generalized linear regressions. It is rarely discussed in regression analysis for panel count data. One advantage of Bayesian analysis is that the predictive inference automatically accounts for parameter uncertainties. Consider a future subject with covariates $\tilde{\mathbf{x}}$. We are interested in a predictive distribution of the count \tilde{y} during a pre-specified time period \mathbb{T} . Let \mathbb{D} represent all past data and let $\boldsymbol{\xi}$ represent all parameters in the model. Then the posterior predictive

distribution for \tilde{y} is

$$p(\tilde{y} | \mathbb{D}, \tilde{\mathbf{x}}) = \int_{\mathbb{D}} p(\tilde{y} | \boldsymbol{\xi}, \tilde{\mathbf{x}}) p(\boldsymbol{\xi} | \mathbb{D}) d\boldsymbol{\xi}.$$

As long as we have posterior samples from $p(\boldsymbol{\xi} | \mathbb{D})$, this predictive distribution is computationally available. Suppose we have $b = 1, \dots, B$ posterior samples from MCMC, that is, we have $\boldsymbol{\xi}^{(b)}$ containing $\lambda_0^{(b)}(\cdot)$, $\boldsymbol{\beta}^{(b)}$ and $\mathbf{D}^{(b)}$. We can proceed as follows: for each b ,

1. Draw $\tilde{u}^{(b)}$ from $\text{lognormal}(0, D_{22}^{(b)})$.
2. Draw $\tilde{y}^{(b)}$ from $\text{Poi}(\tilde{E}^{(b)})$, with $\tilde{E}^{(b)} = \exp\{\tilde{\mathbf{x}}' \boldsymbol{\beta}^{(b)}\} \tilde{u}^{(b)} \int_{\mathbb{T}} \lambda_0^{(b)}(t) dt$.

Then, $\tilde{y}^{(1)}, \dots, \tilde{y}^{(B)}$ is a sample from the correct predictive distribution. Note that the prediction is made marginally on the event process as the observation time period \mathbb{T} is pre-specified. Prediction of observation times is rarely of interest, but possible under this model. A medical practitioner may be interested in a probability of no recurrence in \mathbb{T} , given the subject's covariates, and that is $P(\tilde{y} = 0 | \mathbb{D}, \tilde{\mathbf{x}})$, computed from the predictive distribution.

5 Simulation

Our proposed Bayesian inference can simultaneously estimate regression coefficients and baseline intensity functions with allowing for correlated processes. There was no previous work that handles such a complicated scenario in a single model. In this simulation section, we compare our proposed inference with existing approaches which give different types of partial results. The simulation section is designed as two sub-themes. Theme 1 is that we compare our method with HSW (Hu et al., 2003) and ZTS (Zhao, Tong and Sun, 2013) on estimation of regression parameters. Both work focused on estimating regression parameters alone without estimating baseline functions. Theme 2 is that we compare our method with YWH (Yao et al., 2016) on estimation of cumulative baseline functions. YWH used monotone splines for cumulative baseline functions, however, did not consider a dependent observation process.

5.1 Comparing estimation of regression coefficients

In Theme 1, we compare estimation of regression parameters between our method and those from HSW and ZTS under two simulation settings:

1. Setting 1 represents an original case that was considered in ZTS, where our model and the one in HSW are both misspecified. Baseline intensity functions are $\mu_0(t) = 1/8$ and $\lambda_0(t) = 1/t$. The censoring times C_i are generated from $\text{Unif}(2, 9)$. The frailties are generated as $u_i^O \sim \text{Ga}(2, 0.2)$ and $u_i^N = (u_i^O)^{0.5} + \text{Ga}(1, 2)$. Let x_i be from Bernoulli with probability 0.5 and let $\beta = \gamma = 1$. Sample size is set to be $n = 100$.
2. Setting 2 represents a case for which none of the three models is misspecified. Baseline intensity functions are $\mu_0(t) = 0.25\{\exp(-t/20) + 0.5 \exp[-((t-70)/40)^2]\}$ and $\lambda_0(t) = 0.125\{\exp(-t/10) + 0.5 \exp[-((t-70)/20)^2]\}$. The censoring times C_i are generated from $\text{Unif}(50, 100)$. The frailties are generated independently from lognormal with zero mean and 0.25 variance. Let x_i be from $\text{Unif}(0, 1)$ and let $\beta = \gamma = 1$. Sample size is set to be $n = 100$.

For each setting we generated 500 datasets and applied all three methods to the same datasets. For our proposed method, we set $\nu = 2.5$ in the Matérn kernel as a balanced choice for differentiability. To obtain fast convergence in each replication of the simulation study, we pre-fixed $\theta_1 = \theta_2 = 0.5$ for Setting 1 and $\theta_1 = \theta_2 = 4$ for Setting 2. The choice of hyperparameters will not drastically change the estimation, as shown in a sensitivity analysis in Section 6. In each replication of the 500 datasets, we ran the MCMC algorithm for 20,000 iterations with a burn-in size of 5,000. Since β , of the event process, is usually of primary interest, and note that γ is not available in ZTS, we compare the estimated bias, root mean squared errors (RMSE) and 95% coverage probabilities (CP) for β only. The comparison results are presented in Table 1. It can be seen that all three methods result in small biases, reasonable RMSE and CP. However, our proposed method outperforms HSW and ZTS under both settings.

5.2 Comparing estimation of baseline functions

In Theme 2, we compare our method with the method in YWH, in particular on estimation of cumulative baseline functions. Our method provides both intensity and cumulative intensity estimation under dependent frailties, and hence is more general than YWH. We used the R package “PCDSpline” developed by YWH to implement their method. Consider the following setting for simulating panel count data.

3. Baseline intensity functions are $\mu_0(t) = 0.25 \exp\{-t/100\}$ and $\lambda_0(t) = 0.25 \exp\{-(t-20)^2/25\} + 0.25 \exp\{-(t-50)^2/25\} + 0.25 \exp\{-(t-80)^2/25\}$. The censoring times $C_i = 100$ are fixed for all subjects. The frailties are generated from a bivariate lognormal

with zero mean and covariance matrix $D_{11} = D_{22} = 0.25$ and $D_{12} = 0.125$. Let x_{1i} and x_{2i} both be from $\text{Unif}(0, 1)$ and let $\beta_1 = \gamma_1 = -1$ and $\beta_2 = \gamma_2 = 1$. Sample size is set to be $n = 100$.

We generated 500 datasets and applied both methods to the same datasets. For the method in YWH, we used both linear bases and quadratic bases for the spline model, with 10 equally spaced knots following the recommendation in YWH. For our proposed method, we set $\nu = 2.5$ and pre-fixed $\theta_1 = 4$ and $\theta_2 = 2$ for the same reasons stated in Section 5.1. In each replication of the 500 datasets, we ran the MCMC algorithm for 20,000 iterations with a burn-in size of 5,000. We compare estimates on regression parameter β and a rescaled cumulative intensity function $\Lambda_0(t) = \int_0^t \lambda_0(s)ds / \int_0^T \lambda_0(s)ds$ over the time region $[0, T]$. Table 2 shows biases, RMSE and CP for β and $\Lambda_0(t)$ on four interior time points within the region $[0, 100]$. Figure 2 shows point-wise comparisons of biases and RMSE over the region $[0, 100]$. It can be seen that our proposed method performs better with smaller biases and RMSE, and more reasonable CP than those given by YWH. In addition, Figure 3 shows averaged estimates of $\lambda_0(t)$, $\mu_0(t)$ and their cumulative functions based on 500 replicates, together with their true curves. These averaged estimates match their true curves extremely well.

6 Skin Cancer Data

The skin cancer data were analyzed in Li et al. (2011) and Yao et al. (2016). A chemoprevention trial for skin cancer patients were conducted by the University of Wisconsin Comprehensive Cancer Center. The aim was to evaluate the effectiveness of the $0.5 \text{ g/m}^2/\text{day}$ DFMO treatment in reducing recurrent tumors for patients with non-melanoma skin cancers. The study consists of 291 patients (with one removal) in total, who were then randomized into a placebo group (147) and a treatment group (144). Two types of cancer, basal cell carcinoma and squamous cell carcinoma, were combined in this analysis. Two covariates, the treatment indicator and the number of initial tumors, were included in this analysis. We chose hyperparameters in the GP as follows: let $\nu = 1.5$ in the Matérn kernel and $\theta_k \sim \text{Ga}(4, 4)$ for $k = 1, 2$. We ran MCMC with randomly picked initial values for 200,000 iterations with a 50,000 burn-in size. Convergence diagnostics are given in a supplementary file.

Regression parameters are estimated as follows: posterior mean (s.d.) of β_1 (DFMO) is -0.104 (0.149) and posterior mean (s.d.) of β_2 (Initial tumor number) is 0.111 (0.012), which indicates that the DFMO treatment effect is marginal but the initial number of tumors has

a significant positive effect on tumor recurrences. These numbers are in general consistent with conclusions in Li et al. (2011). Figure 4 shows posterior means and credible bands of $\lambda_0(t)$ and $\mu_0(t)$. Comparing the estimated observation intensity with the sample observation times, our estimate well represents the shape and pattern in sample data. Notice that there is a clear periodic pattern in observation times, which is due to that the original clinical trial planned scheduling follow-up times every six months, however, each patient’s actual visit times appear to be random and do not match the schedule exactly.

Though the same data have been analyzed in literature, results for prediction do not seem available. Suppose that we are interested in predicting the recurrence count within five years after the initial treatment for a future subject, and we are also interested in the probability of no recurrence, a.k.a. free of disease, within five years after treatment. We argue that this is an important piece of information for both physicians and patients. Figure 5 shows Bayesian predictive distributions for various combinations of covariates. Figure 6 shows Bayesian predictive probabilities of the five-year-disease-free event.

As a model checking step, we considered a sensitivity analysis for difference choices of hyperparameters. We considered three different settings: (1) $\nu = 2.5$, $\theta_k \sim \text{Ga}(8, 4)$; (2) $\nu = 1.5$, $\theta_k \sim \text{Ga}(4, 4)$; and (3) $\nu = 0.5$, $\theta_k \sim \text{Ga}(16, 4)$, $k = 1, 2$. For each setting, we ran MCMC for 200,000 iterations with a 50,000 burn-in size. Estimates of β , γ and $\Lambda_0(t)$ are compared in Table 3 and Figure 7. The results show that the estimation is quite robust with respect to the choice of hyperparameters. These choices, however, do change the differentiability and smoothness of the estimated curves. To choose between different hyperparameter values, one may consider model selection criteria, such as the deviance information criterion (DIC). We report the DIC in Table 3 and in this comparison, Choice 2 is preferred with the smallest DIC value.

7 Discussion

In this paper, we developed a bivariate log-Gaussian Cox process model for panel count data. We derived inference and computation procedures for the proposed model. We emphasized the need of smooth estimation of intensity functions and discussed prediction in panel count data analysis. One issue of using the Gaussian process model is learning the scale parameter θ in the kernel, which determines smoothness of the Gaussian process. It is known that the point process data often provide only weak information about θ . We used a fully Bayesian solution with informative priors so that the posterior is balanced between data information and user’s information. On the other hand, an empirical Bayes approach, by maximizing

the marginal likelihood of θ , is worth future investigations.

A potential advantage of using Gaussian process models for the baseline intensity function is that this specification can be useful for modelling multivariate panel count data. Consider that a patient is monitored for multiple events simultaneously, which is not uncommon in a medical study. For instance, in a clinical trial for assessing influenza vaccines (Zaman et al., 2008), each patient was monitored for multiple symptoms, such as fever, cough and diarrhea. Since all these symptoms are influenza-related, the underlying intensity patterns may be highly correlated. If we assume K nonhomogeneous Poisson processes for the multiple events, each intensity function can be modelled by $\lambda_{ik}(t) = \lambda_{0k}(t) \exp\{\mathbf{x}'_i \boldsymbol{\beta}_k\} u_{ik}$, $k = 1, \dots, K$ and $i = 1, \dots, n$. To model the underlying dependence between multiple events, let $g_k(t) = \log \lambda_{0k}(t)$ and consider that $(g_1(t), \dots, g_K(t))$ jointly be a multivariate Gaussian process, with the cross-covariance function between $g_j(t)$ and $g_k(t)$ being $C_{jk}(h) = \text{Cov}\{g_j(t), g_k(t+h)\}$. Then, the cross-covariance between $\lambda_{ij}(t)$ and $\lambda_{ik}(t)$ (for subject i) becomes

$$\text{Cov}\{\lambda_{ij}(t), \lambda_{ik}(t+h)\} = \text{E}\{\lambda_{ij}(t)\} \text{E}\{\lambda_{ik}(t)\} [\exp\{C_{jk}(h) + D_{jk}\} - 1],$$

where $C_{jk}(h)$ controls the degree of similarity between the two intensity functions and D_{jk} controls the dependence of the overall intensity magnitude. In the multivariate extension described above, the Gaussian process specification is useful to accommodate various dependence structures.

Acknowledgement

The computing for this project was performed at the OSU High Performance Computing Center at Oklahoma State University supported in part through the National Science Foundation grant OCI-1126330. We thank an associate editor and a referee for their valuable comments to the earlier version of this manuscript.

References

- Altman, D. and Royston, P. (2000), ‘What do we mean by validating a prognostic model?’, *Statistics in Medicine* **19**, 453–473.
- Anderson, P. and Gill, R. (1982), ‘Cox regression model for counting processes: A large sample study’, *The Annals of Statistics* **10**, 1100–1120.

- Diggle, P., Moraga, P., Rowlingson, B. and Taylor, B. (2013), ‘Spatial and spatio-temporal log-Gaussian Cox processes: extending the geostatistical paradigm’, *Statistical Science* **28**, 542–563.
- Gilks, W. and Wild, P. (1992), ‘Adaptive rejection sampling for Gibbs sampling’, *Applied Statistics* **41**, 337–348.
- Girolami, M. and Calderhead, B. (2011), ‘Riemann manifold Langevin and Hamiltonian Monte Carlo’, *Journal of the Royal Statistical Society, Series B* **73**, 123–214.
- He, X., Tong, X. and Sun, J. (2009), ‘Semiparametric analysis of panel count data with correlated observation and follow-up times’, *Lifetime Data Analysis* **15**, 177–196.
- Hu, X., Sun, J. and WEI, L. (2003), ‘Regression parameter estimation from panel counts’, *Scandinavian Journal of Statistics* **30**, 25–43.
- Hua, L. and Zhang, Y. (2012), ‘Spline-based semiparametric projected generalized estimating equation method for panel count data’, *Biostatistics* **13**(3), 440–454.
- Hua, L., Zhang, Y. and Tu, W. (2014), ‘A spline-based semiparametric sieve likelihood method for over-dispersed panel count data’, *Canadian Journal of Statistics* **42**(2), 217–245.
- Huang, C., Wang, M. and Zhang, Y. (2006), ‘Analyzing panel count data with informative observation times’, *Biometrika* **93**, 763–775.
- Kalbfleisch, J. and Prentice, R. (2011), *The Statistical Analysis of Failure Time Data*, John Wiley & Sons.
- Kimeldorf, G. and Wahba, G. (1970), ‘A correspondence between Bayesian estimation on stochastic processes and smoothing by splines’, *The Annals of Mathematical Statistics* **41**, 495–502.
- Li, N., Park, D., Sun, J. and K, K. (2011), ‘Semiparametric transformation models for multivariate panel count data with dependent observation process’, *The Canadian Journal of Statistics* **39**, 458–474.
- Li, N., Sun, L. and Sun, J. (2010), ‘Semiparametric transformation models for panel count data with dependent observation process’, *Statistics in Biosciences* **2**, 191–210.

- Li, Y., He, X., Wang, H., Zhang, B. and Sun, J. (2015), ‘Semiparametric regression of multivariate panel count data with informative observation times’, *Journal of Multivariate Analysis* **140**, 209–219.
- Lu, M., Zhang, Y. and Huang, J. (2007), ‘Estimation of the mean function with panel count data using monotone polynomial splines’, *Biometrika* **94**(3), 705–718.
- Lu, M., Zhang, Y. and Huang, J. (2009), ‘Semiparametric estimation methods for panel count data using monotone b-splines’, *Journal of the American Statistical Association* **104**(487), 1060–1070.
- Møller, J., Syversveen, A. and Waagepetersen, R. (1998), ‘Log Gaussian Cox processes’, *Scandinavian Journal of Statistics* **25**, 451–482.
- Mostafa, M. and Mahmoud, M. (1964), ‘On the problem of estimation for the bivariate lognormal distribution’, *Biometrika* **51**, 522–527.
- Neal, R. (2010), MCMC using Hamiltonian dynamics, in Brooks, Gelman, Jones and Meng, eds, ‘Handbook of Markov Chain Monte Carlo’, Chapman and Hall - CRC Press.
- Nielsen, J. and Dean, C. (2008), ‘Clustered mixed nonhomogeneous poisson process spline models for the analysis of recurrent event panel data’, *Biometrics* **64**, 751–761.
- Rasmussen, C. and Williams, C. (2006), *Gaussian Processes for Machine Learning*, MIT press Cambridge.
- Royston, P. and Altman, D. (2013), ‘External validation of a cox prognostic model: principles and methods’, *BMC Medical Research Methodology* **13**, 33.
- Sun, J., Tong, X. and He, X. (2007), ‘Regression analysis of panel count data with dependent observation times’, *Biometrics* **63**, 1053–1059.
- Sun, J. and Wei, L. (2000), ‘Regression analysis of panel count data with covariate-dependent observation and censor times’, *Journal of the Royal Statistical Society, Series B* **62**, 293–302.
- Yao, B., Wang, L. and He, X. (2016), ‘Semiparametric regression analysis of panel count data allowing for within-subject correlation’, *Computational Statistics & Data Analysis* **97**, 47–59.

- Zaman, K., Roy, E., Arifeen, S. E., Rahman, M., Raqib, R., Wilson, E., Omer, S. B., Shahid, N. S., Breiman, R. F. and Steinhoff, M. C. (2008), ‘Effectiveness of maternal influenza immunization in mothers and infants’, *New England Journal of Medicine* **359**, 1555–1564.
- Zhao, H., Li, Y. and Sun, J. (2013), ‘Analyzing panel count data with a dependent observation process and a terminal event’, *Canadian Journal of Statistics* **41**, 174–191.
- Zhao, X., Tong, X. and Sun, J. (2013), ‘Robust estimation for panel count data with informative observation times’, *Computational Statistics & Data Analysis* **57**, 33–40.
- Zhou, J., Zhang, H. and Sun, L. (2016), ‘Joint analysis of panel count data with an informative observation process and a dependent terminal event’, *Lifetime Data Analysis* pp. 1–25.

Table 1: Simulation: Compare regression parameter estimation with HSW(2003) and ZTS(2013). RMSE: root mean squared error. CP: 95% coverage probability. Bayesian approach uses a symmetric credible interval.

	Setting 1								
	Proposed			HSW			ZTS		
	Bias	RMSE	CP	Bias	RMSE	CP	Bias	RMSE	CP
$\beta = 1$ (Event)	-0.004	0.097	0.94	0.005	0.195	0.96	0.006	0.221	0.92
	Setting 2								
	Proposed			HSW			ZTS		
	Bias	RMSE	CP	Bias	RMSE	CP	Bias	RMSE	CP
$\beta = 1$ (Event)	-0.002	0.255	0.95	0.017	0.328	0.96	0.018	0.332	0.96

Table 2: Simulation Setting 3: Compare with YWH(2016). RMSE: root mean squared error. CP: 95% coverage probability. Bayesian approach uses a symmetric credible interval.

	Proposed			YWH Linear			YWH Quadratic		
	Bias	RMSE	CP	Bias	RMSE	CP	Bias	RMSE	CP
$\beta_1 = -1$	0.012	0.226	0.96	0.015	0.236	0.85	0.007	0.238	0.85
$\beta_2 = 1$	0.002	0.238	0.95	-0.015	0.235	0.76	-0.005	0.238	0.76
$\Lambda_0(20)$	0.0004	0.016	0.94	0.036	0.039	-	-0.056	0.056	-
$\Lambda_0(40)$	0.0009	0.017	0.97	-0.000	0.017	-	0.027	0.032	-
$\Lambda_0(60)$	-0.004	0.018	0.94	-0.016	0.024	-	-0.032	0.037	-
$\Lambda_0(80)$	-0.002	0.019	0.95	-0.051	0.054	-	0.047	0.048	-

Table 3: Skin cancer data: Sensitivity analysis and DIC. Compare hyperparameter choices: (1) $\nu = 2.5$, $\theta_k \sim \text{Ga}(8, 4)$; (2) $\nu = 1.5$, $\theta_k \sim \text{Ga}(4, 4)$; and (3) $\nu = 0.5$, $\theta_k \sim \text{Ga}(16, 4)$, $k = 1, 2$. Table shows posterior means and standard deviations.

	β_1	β_2	γ_1	γ_2	DIC
Choice 1	-0.105 (0.149)	0.111 (0.012)	-0.0374 (0.0462)	0.00844 (0.00407)	20783.1
Choice 2	-0.104 (0.149)	0.111 (0.012)	-0.0370 (0.0462)	0.00846 (0.00407)	20766.0
Choice 3	-0.102 (0.149)	0.111 (0.012)	-0.0373 (0.0462)	0.00848 (0.00409)	20799.2

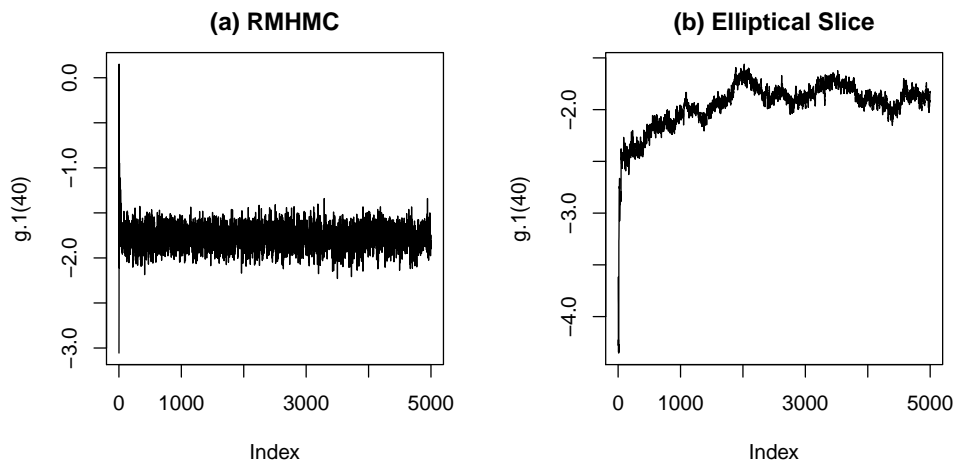


Figure 1: (a). Convergence of $g_1(40)$ using RMHMC. (b). Convergence of $g_1(40)$ using elliptical slice sampling. Two sampling techniques are compared with random initial values for the first 5000 iterations using the skin cancer data.

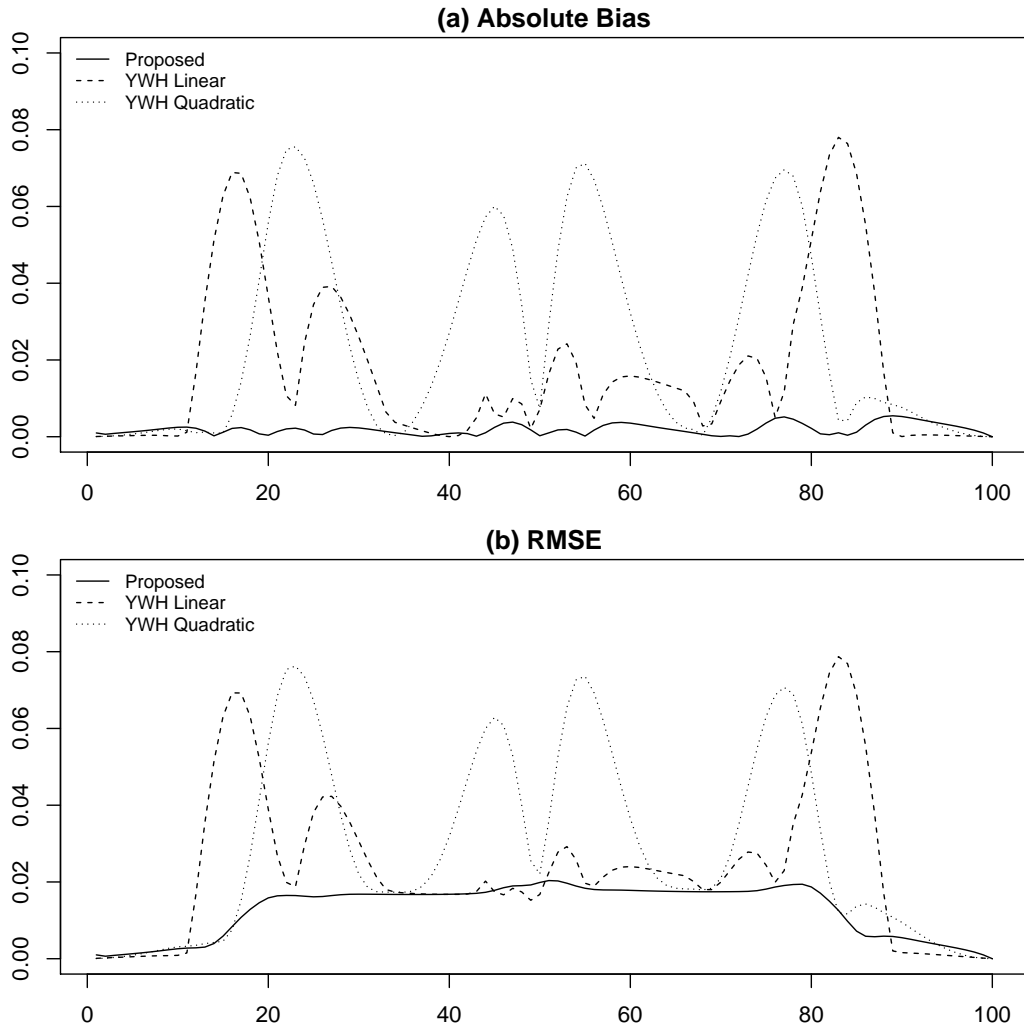


Figure 2: Simulation setting 3: (a). absolute bias of $\widehat{\Lambda}_0(t)$. (b). RMSE of $\widehat{\Lambda}_0(t)$.

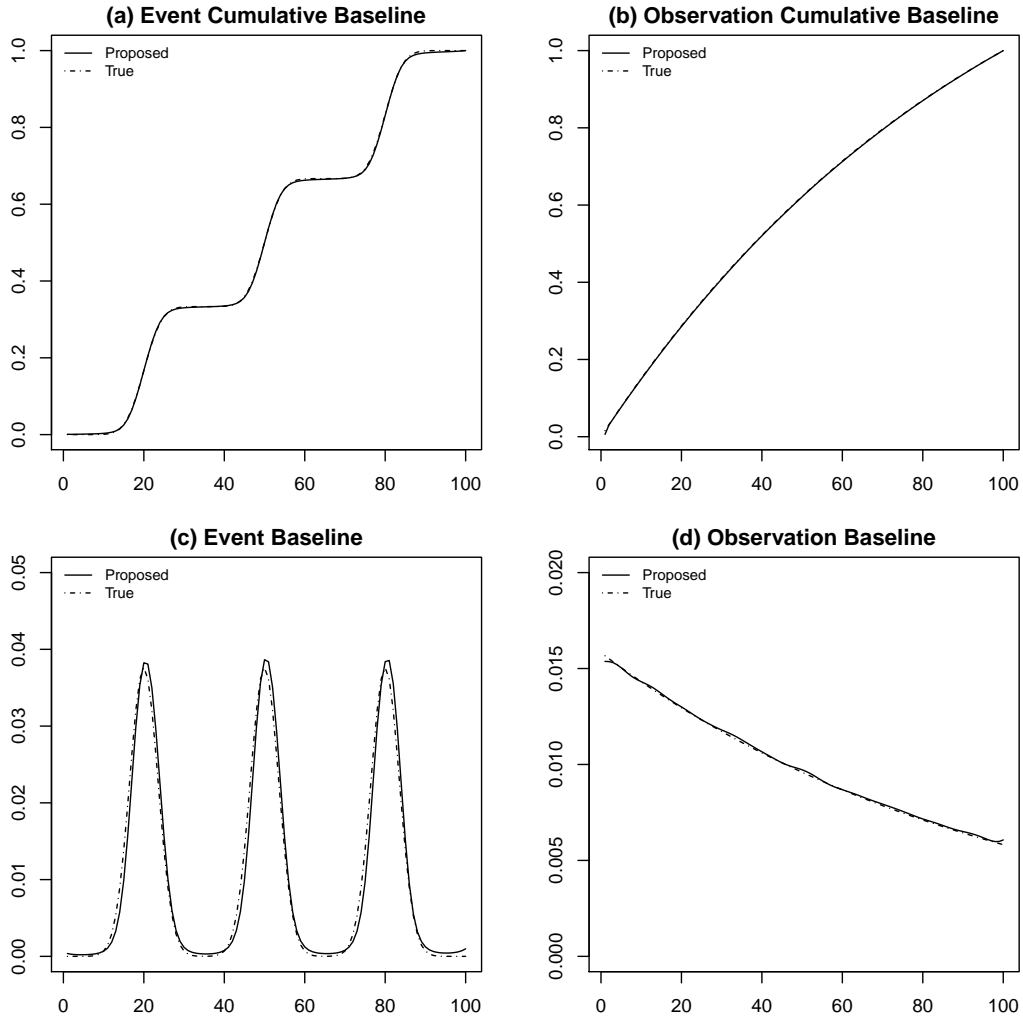


Figure 3: Simulation Setting 3: Average fit of 500 replicates. (a). Cumulative function of $\lambda_0(t)$. (b). Cumulative function of $\mu_0(t)$. (c). $\lambda_0(t)$. (d). $\mu_0(t)$.

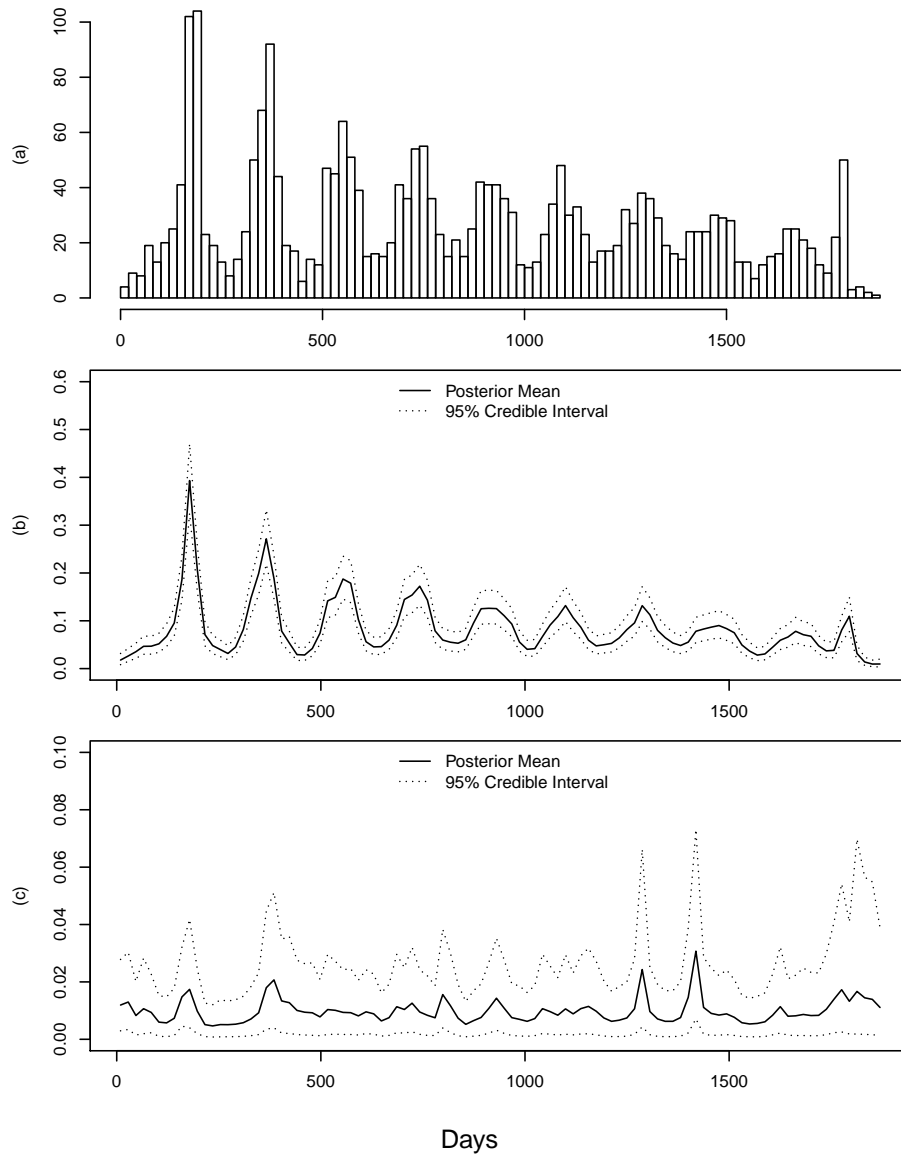


Figure 4: Skin cancer data: (a). Actual observation times of all patients. (b). Posterior observation intensity $\mu_0(t)$. (c). Posterior event intensity $\lambda_0(t)$.

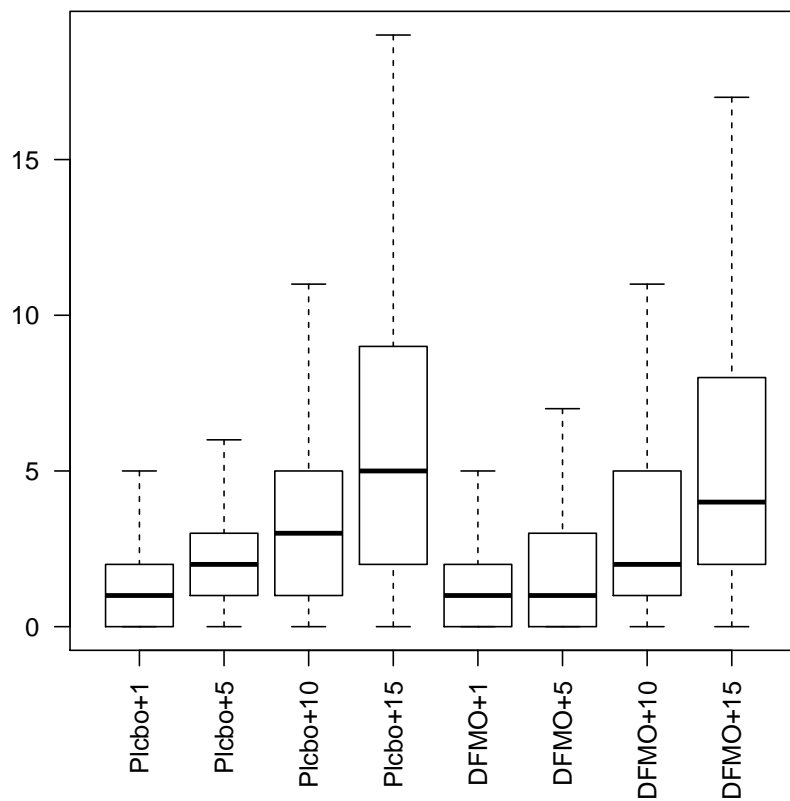


Figure 5: Skin cancer data: Predictive distributions for the tumor recurrence count \tilde{y} in five years after treatment. Distributions are displayed for different covariates $\tilde{\mathbf{x}}$. “DFMO+5” means the future subject has 5 initial tumors and is treated with DFMO. Outliers beyond 1.5 Interquartile Quartile Range are not displayed.

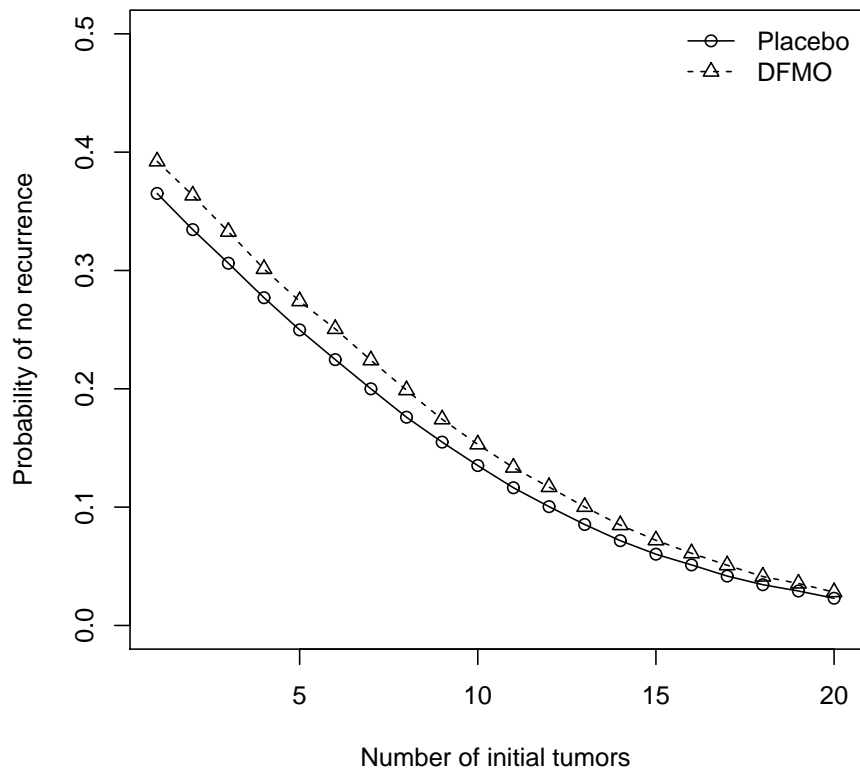


Figure 6: Skin cancer data: Predictive probability of no recurrence of skin cancer (disease-free) within five years of treatment: $P(\tilde{y} = 0 \mid \mathbb{D}, \mathbb{T}, \tilde{\mathbf{x}})$.

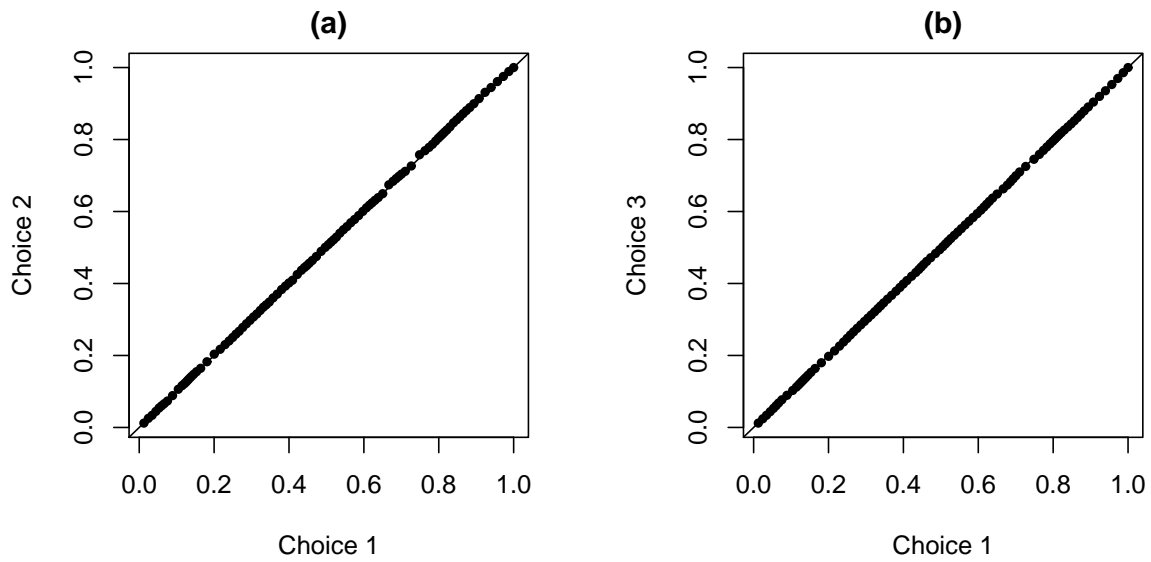


Figure 7: Skin cancer data: Sensitivity analysis for the posterior mean estimate of $\Lambda_0(t)$. Compare hyperparameter choices: (1) $\nu = 2.5$, $\theta_k \sim \text{Ga}(8, 4)$; (2) $\nu = 1.5$, $\theta_k \sim \text{Ga}(4, 4)$; and (3) $\nu = 0.5$, $\theta_k \sim \text{Ga}(16, 4)$, $k = 1, 2$.